Journal of Magnetism and Magnetic Materials 369 (2014) 243–248

Contents lists available at ScienceDirect

Journal of Magnetism and Magnetic Materials

journal homepage: www.elsevier.com/locate/jmmm

Magnetic ordering of $ScMn_6Ge_6$ by neutron diffraction

P. Schobinger-Papamantellos [a,*], J. Rodríguez-Carvajal [b], K.H.J. Buschow [c]

[a] Laboratory of Crystallography, ETH-Zürich, 8093 Zürich, Switzerland
[b] Institut Laue-Langevin, CS 20156, 38042 Grenoble Cedex, France
[c] Van der Waals-Zeeman Institute, University of Amsterdam, NL-1018 XE The Netherlands

ARTICLE INFO

Article history:
Received 30 April 2014
Received in revised form
19 June 2014
Available online 27 June 2014

Keywords:
Incommensurate magnetic structure
Magnetic structure refinement
Neutron diffraction
Intermetallic germanides

ABSTRACT

The compound $ScMn_6Ge_6$ ($HfFe_6Ge_6$-type, *P6/mmm*) orders antiferromagnetically below $T_N=516$ K. Neutron powder diffraction at various temperatures 1.5–309 K shows the existence of two distinct magnetic ordering ranges described by the commensurate $\mathbf{q}_1=(0, 0, 1/2)$ and the incommensurate $\mathbf{q}_2=(0, 0, q_z)$ vectors: (i) the *HT* (high temperature) $T_t \approx 100\ \mathrm{K} < T < 309\ \mathrm{K}$ range described by $\mathbf{q}_1$, corresponds to an easy axis antiferromagnetic stacking of the Mn ferromagnetic (0 0 1) layers (+ − − +) at $z_{Mn} \sim 1/4, 3/4, 5/4, 7/4$, the Mn moments being confined to the *c*-axis. (ii) The *LT* (low temperature) $T_t > T > 1.5$ K range has an easy double-cone incommensurately modulated structure described by two vectors ($\mathbf{q}_1$, $\mathbf{q}_2$). At 1.5 K $\mathbf{q}_2=(0, 0, 0.405(1))$, the spiral angle is $\Phi=145.8^\circ$ the cone half angle is $\alpha \approx 8^\circ$ and the ordered moment value $\mu_{Mn}=2.12(2)\ \mu_B$ is the same as for the isomorphic RMn_6Ge_6 (R=heavy rare earth) compounds. The 1.5 K $\mathbf{q}_2$ satellites are very weak as the in-plane moment component measures only 0.31 μ_B.

1. Introduction

The magnetic properties of various RMn_6Ge_6 hexagonal heavy rare earth (R) compounds of $HfFe_6Ge_6$ structure type (*P6/mmm*) [1,2] have been reported by Venturini et al. [3]. RMn_6Ge_6 compounds have high ordering temperatures in the range 400–520 K and undergo various sequences of spin reorientation transitions indicating the presence of complex competing magnetic interactions. $LuMn_6Ge_6$ [4] as well as the high temperature (*HT*) phase of the compounds RMn_6Ge_6 (R=Y, Er, Ho and Tm) [5–8] were reported to have a uniaxial antiferromagnetic arrangement of the Mn moments parallel to the *c*-axis, associated with the wave vector $\mathbf{q}=(0, 0, 1/2)$ and a cell doubling along *c*. The present authors reported a similar behaviour for $ScMn_6Ge_6$ in [4]. A later preliminary study [9] reports an ordered Mn moment value of $\mu_{Mn}=1.94\ \mu_B$ at 300 K for $ScMn_6Ge_6$ and the occurrence of a spin reorientation transition below $T_t=255$ K with the wave vector $\mathbf{q}_2=(0, 0, q_z)$ associated with a simultaneous strong decrease of the $\mathbf{q}_1$ magnetic satellites in favour of the $\mathbf{q}_2$ satellites. However no details about the nature of the *LT* incommensurate ($\mathbf{q}_1$, $\mathbf{q}_2$) phase were given.

In the present investigation we report on the magnetic ordering of the compound $ScMn_6Ge_6$ on the basis of neutron diffraction data at various temperatures. Our results confirm the findings concerning the *HT* uniaxial antiferromagnetic ordering type $\mathbf{q}_1=(0, 0, 1/2)$ and the occurrence of a spin reorientation at a lower temperature [9] and completes the data analysis of the *LT* incommensurately modulated structure.

Using the present opportunity a correction by a factor 2 of the Mn moment values given by us in [4,6–8] has to be introduced for the $\mathbf{q}_1=(0, 0, 1/2)$ phase for RMn_6Ge_6 (R=Lu, Ho, Er, Tm). As pointed out also in [9] this is due to the erroneously use of the nuclear structure scale factor (sc) instead of sc 0.25 as the magnetic intensity calculations were carried out in the commensurate (*a*, *b*, 2*c*) cell.

2. Neutron diffraction

The $ScMn_6Ge_6$ powder sample used for the neutron diffraction study was prepared by arc melting materials of at least 99.9% purity. After arc melting the sample was wrapped in Ta foil and placed in an evacuated quartz tube and vacuum annealed at 800 °C as reported in [10]. According to macroscopic magnetic measurements [3] $ScMn_6Ge_6$ orders antiferromagnetically at $T_N=516$ K and displays a Curie–Weiss behaviour above T_N. The high value of the paramagnetic Curie temperature $\theta_p=500$ K indicates the presence of strong ferromagnetic interactions. The paramagnetic manganese moment value is $\mu_{eff}(Mn)=3.05\ \mu_B$.

The sample was investigated using the facilities of the Orphée reactor (LLB-Saclay) for several temperatures with a T-window of

* Corresponding author. Tel.: +41 44 632 3773; fax: +41 44 632 1133.
E-mail address: Schobinger@mat.ethz.ch (P. Schobinger-Papamantellos).

http://dx.doi.org/10.1016/j.jmmm.2014.06.052
0304-8853/

50 K for 1.5–309 K. The data were collected on the G4.1 diffractometer (800 cells multidetector). The step increment in 2θ was 0.1°. The data were analysed with the programme *FullProf* [11]. The plots of the magnetic structures were done with the programme *FullProf Studio* [12]. All refinements led to reliability factors R_n (nuclear), R_m (magnetic) values around 2% and 6–8% and R_{wp} (profile) 16%. The sample was found to contain small amounts of impurity phases and numerous binary and ternary phases of the Sc–Mn–Ge phase diagram [13] were used in the impurity search. The strongest impurity peaks at $2\theta \approx 44°$, 51° and 75° denoted by lines in Fig. 1a were identified as elemental Ge (8%) and were included in the refinements together with some minor peaks of the $ScMnGe_2$ (3%) compound.

2.1. The magnetic structure in the range 100 K < T < 309 K: AF ($\mathbf{q}_1$=(0, 0, 1/2))

The 149 K and 309 K (cf. Fig. 1) neutron patterns obtained in the magnetically ordered range show as expected [4,9], next to the nuclear reflections, a single set of magnetic reflections associated with the wave vector $\mathbf{q}_1$=(0, 0, 1/2). The fact that all (0, 0, l) $\pm\mathbf{q}_1$ reflections (indicated by arrows in Fig. 1a) have zero intensity suggests a collinear antiferromagnetic arrangement along the c-axis of the Mn magnetic moments (Sc is diamagnetic). The best agreement between observed and calculated values was obtained for an antiparallel stacking of the two (0 0 1) Kagomé layers formed by the Mn atoms at $z \approx 1/4$ and 3/4 (referring to the chemical cell with Sc in the origin (0, 0, 0)) and a sign change when going to the next cell along $\boldsymbol{c}$ of the $\mu_z(+\ -\ -\ +)$ component. The refined 309 K and 149 K ordered moment values are μ_z=1.96(4) and 2.08(4) μ_B/Mn, respectively. An alternative arrangement along c $(++--)$ does not affect the R-factors and the refined parameters due to the fact that the two magnetic structures are strictly equivalent if only the Mn-sublattices are considered (representing a change of the origin). A choice between the two models (which differ in the relative sign of the two Mn-layers "sandwiching" the Sc–Ge layer at z=0) can only be made on the basis of a physical model. The refined parameters given in Table 1 confirm the $HfFe_6Ge_6$ type of structure [1,2]. The values R_n=2.3% and R_m=6.7% at 309 K are satisfactory and indicate no significant deviation of the crystal structure of $ScMn_6Ge_6$ from the basic structure type.

2.2. The LT double cone incommensurately modulated structure: $\mathbf{q}_1$=(0, 0, 1/2) and $\mathbf{q}_2$=(0, 0, q_z)

Neutron diffraction 100 K data cf. Fig. 2a display a single very weak intensity around 10.1° almost indiscernible from the background compared to the 149 K data (Fig. 1b). This reflection is better detectable at 1.5 K on the right side of the (0, 0, 1/2) reciprocal lattice location at 10.22°. It has been indexed as (0 0 1)-$\mathbf{q}_2$ satellite with an incommensurate wave vector along c $\mathbf{q}_2$=(0, 0, q_z) in analogy to the 2 K findings of the isomorphic YMn_6Ge_6 [5] and $LuMn_6Ge_6$ [9] helical structures with q_{2z}=0.385

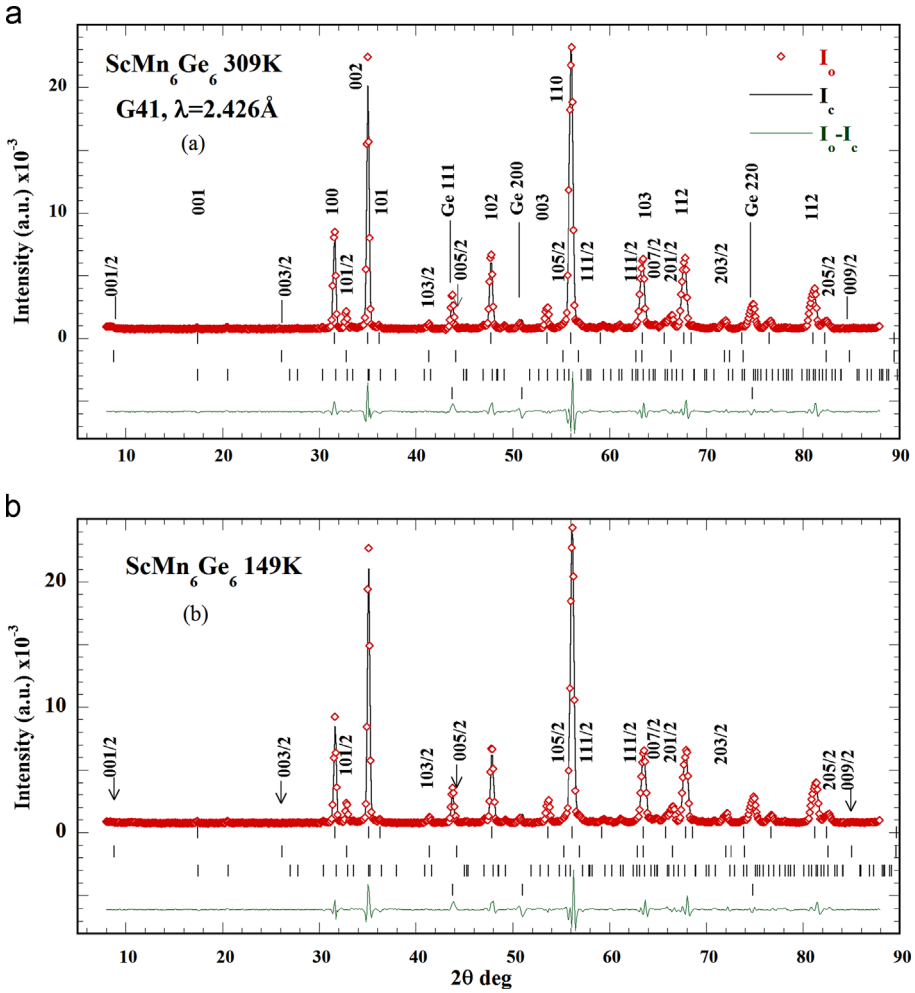

Fig. 1. Observed, calculated and difference neutron diffraction patterns of $ScMn_6Ge_6$ measured at 309 K (top part) and 149 K (bottom part). The location of the absent (0, 0, l/2) $\mathbf{q}_1$ peaks is denoted by arrows.

and 0.402, respectively. The same $\mathbf{q}_2$ orientation was also suggested for $ScMn_6Ge_6$ by the presence of the strong satellite (0 0 0) $\pm\mathbf{q}_2$ in the first Brillouin zone in [9], where the data window was extending below the $2\theta<8^\circ$ limit used in our data.

Table 1
Refined parameters of $ScMn_6Ge_6$ ($HfFe_6Ge_6$-type $P6/mmm$) at 1.5 K, 100 K, 150 K and 309 K. μ_z is the axial Mn moment component associated with the wave vector ($\mathbf{q}_1=(0, 0, 1/2)$). μ_S is the in-plane (0 0 1) spiral moment component for the $\mathbf{q}_2=(0, 0, q_z)$ structure. α_{Mn} is the cone semi-angle of the Mn moments and Φ_S is the spiral angle. μ_T is Mn total moment of the double cone spiral described by the two propagation vectors $\mathbf{q}_1$ and $\mathbf{q}_2$.

Temperature parameter	1.5 K value	100 K value	149 K value	309 K value
Sc at 1*a*: (0, 0, 0)				
z_{Mn} at 6*i*: (1/2, 0, *z*)	0.2457(10)	0.2458(10)	0.2459(10)	0.2458(11)
Ge1 at 2*d*: (1/3, 2/3, 1/2)				
Ge2 at 2*c*: (1/3, 2/3, 0)				
z_{Ge3} at 2*e*: (0, 0, *z*)	0.3387(8)	0.338(1)	0.3387(8)	0.338(1)
Mn: μ_z [μ_B], $\mathbf{q}_1=(0, 0, 1/2)$	2.09(4)	2.10(4)	2.08(4)	1.96(4)
Mn: μ_S [μ_B], $\mathbf{q}_2=(0, 0, q_z)$	0.31(4)	0.16(6)	–	–
α_{Mn} (°)	8(1)	4(1)	–	–
q_z (r.l.u)	0.405(1)	0.411(5)	–	–
Φ_S (°)	145.8	147.9	–	–
Mn: μ_T [μ_B], $\mathbf{q}_1$, $\mathbf{q}_2$	2.12(4)	2.11(4)	2.08(4)	1.96(4)
a (Å)	5.1684(2)	5.1701(2)	5.1727(2)	5.1822(2)
c (Å)	8.0897(4)	8.0914(4)	8.0944(4)	8.1102(4)
R_n (%), *Rm* (%),	2.0, 8.7	2.2, 8.9	2.05, 4.69	2.3, 6.7
R_{wp} (%), R_{exp} (%)	16.4, 3.4	16.5, 4	16.2, 3.3,	16.7, 3.4

As can be seen in Fig. 2b the 1.5 K $\mathbf{q}_1=(0, 0, 1/2)$ intensities remain almost unchanged in contrast to the findings for $ScMn_6Ge_6$ in [9] where they were strongly reduced below $T_t=255$ K. We found that the 1.5 K refined $ScMn_6Ge_6$ $q_{2z}=0.405(1)$ component, corresponding to a spiral angle of $\Phi=2\pi q_z=145.8^\circ$, slightly increases with increasing temperature $1.5\text{ K}<T<100$ K from 0.405(1) to 0.411(5) ($\Phi=147.9^\circ$), respectively. All refinements below 100 K down to 1.5 K are carried out for two distinct vectors as both reflections sets were observed. For $\mathbf{q}_2$ we used a flat spiral model assuming a parallel orientation of the three Mn moments within each (0 0 1) layer by analogy to [5,9]. The refined phase angle between the $z\approx-1/4$, 1/4 Mn (0 0 1) layers is within error close to zero. This means that the Mn spins of the layers $z\approx-1/4$, 1/4 rotate by $2\pi q_{2z}=145.8^\circ$ collectively when going to the next cell i.e. at $z\approx3/4$, 5/4 along the direction of the propagation vector *c*. The refined parameters are summarised for various temperatures in Table 1.

The 1.5 K $ScMn_6Ge_6$ structure corresponds to a double-cone incommensurately modulated magnetic structure described by the vectors $\mathbf{q}_1=(0, 0, 1/2)$ and $\mathbf{q}_2=(0, 0, 0.405)$. It consists of the stacking of ferromagnetic (0 0 1) Mn layers perpendicular to the common direction of the two propagating vectors. The μ_z moment component of the three Mn atoms within the $z\sim1/4$ layer changes sign collectively from cell to cell along *c* and is antiparallel to the Mn moments of the layer $z\sim3/4$. The μ_S in plane spiral component perpendicular to $\mathbf{q}_2=(0, 0, q_z)$ rotates by $\Phi_S=145.8^\circ$ going from cell to cell along *c*.

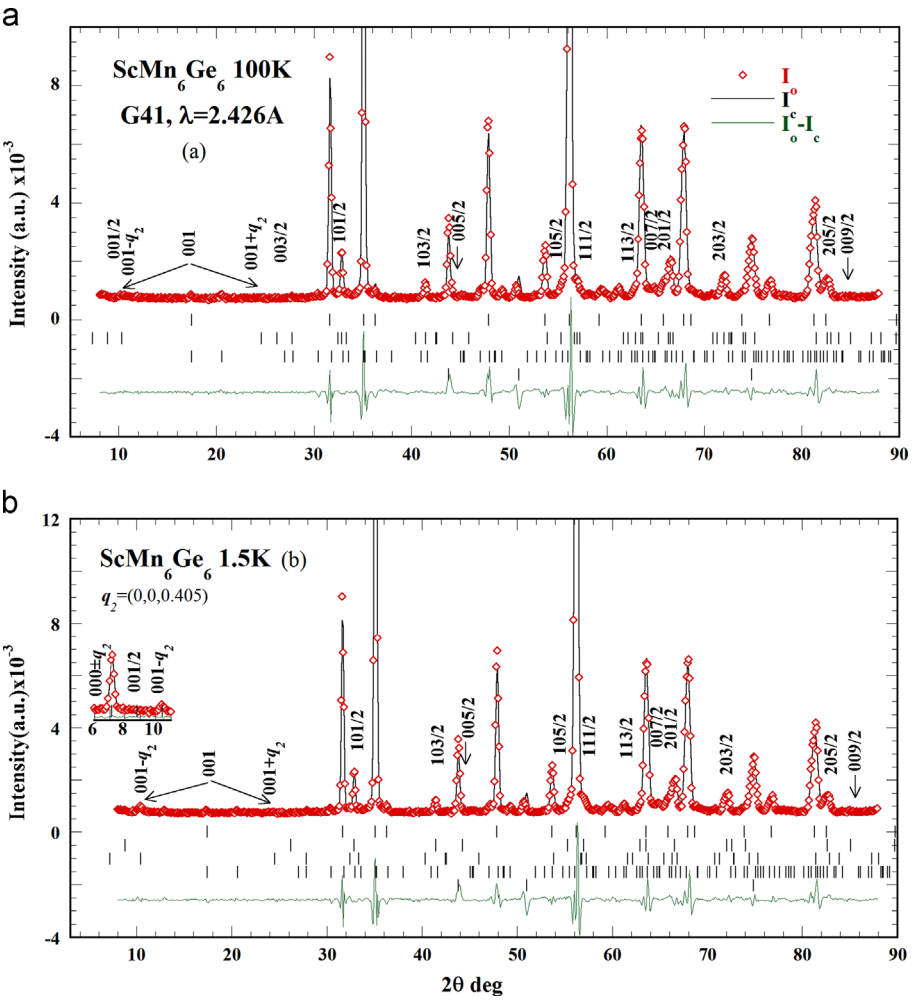

Fig. 2. Observed, calculated and difference of neutron diffraction patterns of $ScMn_6Ge_6$ measured at 100 K and 1.5 K. The inset shows the simulated dominant zero point satellite $000\pm\mathbf{q}_2$ at $2\theta=6.9^\circ$ located outside the low 2θ limit of the 1.5 K data.

The Mn moment amplitude of the ($\mathbf{q}_1$, $\mathbf{q}_2$) structure maintains the same value going from cell to cell along the c-axis and rotates on a very small semicone of $\alpha=8^\circ$ at 1.5 K, as expected from the weak 001-$\mathbf{q}_2$ intensity, and decreases with increasing T to $\alpha=4(1)^\circ$ at 100 K and so does also the spiral moment component. At 150 K the 001-$\mathbf{q}_2$ satellite is no more observable.

The 1.5 K $ScMn_6Ge_6$ incommensurately modulated magnetic structure is shown in Fig. 3 for only 2 cells along c. For the idealised $q_{2z}=0.4=2/5$ value corresponding to a spiral angle $\Phi=144^\circ$ under the action of the $\mathbf{q}_1$ vector the structure becomes commensurate. The Mn moment on the zero cell will return to the origin position after $10\times c$ cells corresponding to a long period commensurate structure of 80.9 Å. This is shown in Figs. 4 and 5 for $5\times c$ cells.

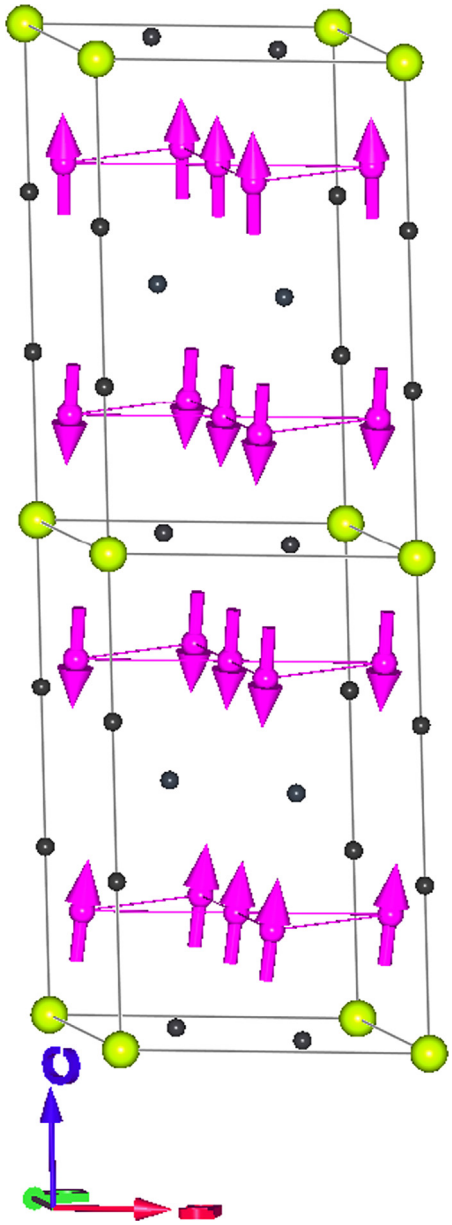

Fig. 3. The double cone incommensurately modulated magnetic structure of the $ScMn_6Ge_6$ compound at 1.5 K for two cells along c described by the vectors $\mathbf{q}_1=(0, 0, 1/2)$ and $\mathbf{q}_2=(0, 0, 0.405)$. The Mn moment resulting by adding up two vertical Fourier components results always in the same value. The Mn moment rotates on a semicone of 8°. The μ_z component changes sign along c by the action of $\mathbf{q}_1$ and μ_S rotates by 145.8° in the plane (0 0 1) by the action of $\mathbf{q}_2$.

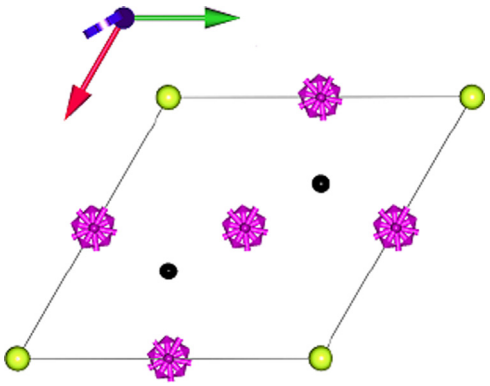

Fig. 4. A (0 0 1) projection of the double-cone incommensurately modulated magnetic structure of the $ScMn_6Ge_6$ compound at 1.5 K for $5\times c$ cells. Showing only $\mathbf{q}_2=(0, 0, 0.4)$ the rotating component. After 5 cells the Mn moment returns to the original position. Considering as well $\mathbf{q}_1$ then the origin orientation will be achieved after $10\times c$ cells.

Fig. 4 displays only the rotating spiral component of the $\mathbf{q}_2$ phase is the (0 0 1) projection. Fixing q_{2z} to the idealised value $q_{2z}=0.4$. In this case the Mn spin returns to its origin location after $5\times c$ cells.

Fig. 5 shows a structure projection with c in the horizontal direction of the 2$\mathbf{q}$-vectors structure, i.e. for $q_{2z}=0.4$ and the simultaneous action of $\mathbf{q}_1=(0, 0, 1/2)$. Fig. 4 was obtained from a calculation where the $\mathbf{q}_1$ and $\mathbf{q}_2$ phases were considered as distinct phases (but only the $\mathbf{q}_2$ phase is shown in this figure) while in Fig. 5 we refined a single phase with both wave vectors.

Various equivalent ways to perform the numerical analysis of 2$\mathbf{q}$-vectors magnetic structures and the derivation of the magnetic structure from the refined Fourier coefficients are extensively described by one of us for the isomorphic $DyMn_6Ge_6$ [14] and in the "*FullProf* examples" showing four different ways of approach for the same compound.

2.3. Thermal evolution of the double cone structure and the Mn spin reorientation

The thermal variation of the refined parameters is displayed in Fig. 6. The Mn total moment value varies between 1.9 μ_B and 2.1 μ_B in the range 309–1.5 K (Fig. 6a) similar to that found in [9] at 300 K. The cell volume in Fig. 6a and the c-axis in Fig. 6b show a slight slope change at 250 K and an almost linear decrease down to 100 K where a further slope change occurs but no more changes below 50 K. The a lattice constant varies within error linearly down to 100 K and changes slope below this temperature (Fig. 6b).

The integrated intensity of the (1 0 1/2) magnetic reflection shows within error no major changes between 309 K and 1.5 K Fig. 6c. One may at most say a slight increase between 309–150 K and very small decrease below 100 K just at the same temperature the 001-q_{2z} satellite becomes detectable in Figs. 2–6c. We suggest that T_t (spin reorientation transition) lies between 100 K and 150 K but not higher [9]. The exact value and nature of the spin reorientation transition require: a narrower T-window, data extending to a lower $2\theta<7^\circ$ angle including the 8× stronger $000\pm\mathbf{q}_2$ satellite (located at 6.977° for $\lambda=2.436$ Å) and very long measuring time. In the inset of Fig. 2b we show the simulated low angle pattern for the parameter values given in Table 1 with the $000\pm\mathbf{q}_2$ satellite. This reproduces the diffraction aspect observed in [9] at 2 K for $ScMn_6Ge_6$.

The spiral angle Φ increases with temperature from 145.8° to 147.9° between 1.5 K and 100 K, while the half cone angle α decreases between 8° and 0° in the same T range. The double cone

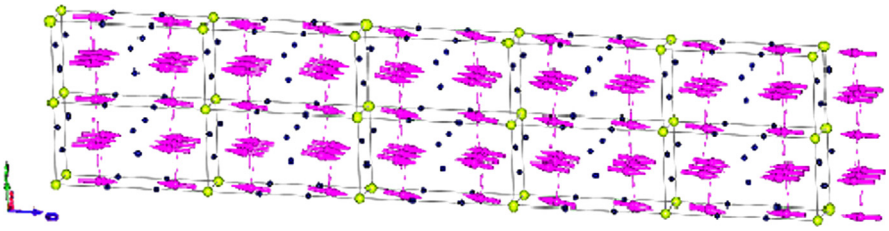

Fig. 5. The axial moment component μ_z changes sign by the action of $\mathbf{q}_1$ and the spiral component μ_S turns by 145.8° by the action of $\mathbf{q}_2$ in the (0 0 1) plane going from cell to cell along *c*. A view of the structure with *c* in the horizontal direction for $5 \times c$ cells. For the commensurate value $\mathbf{q}_2$=(0, 0, 0.4) the structure corresponds to a long period commensurate phase (a, b, $10 \times c$).

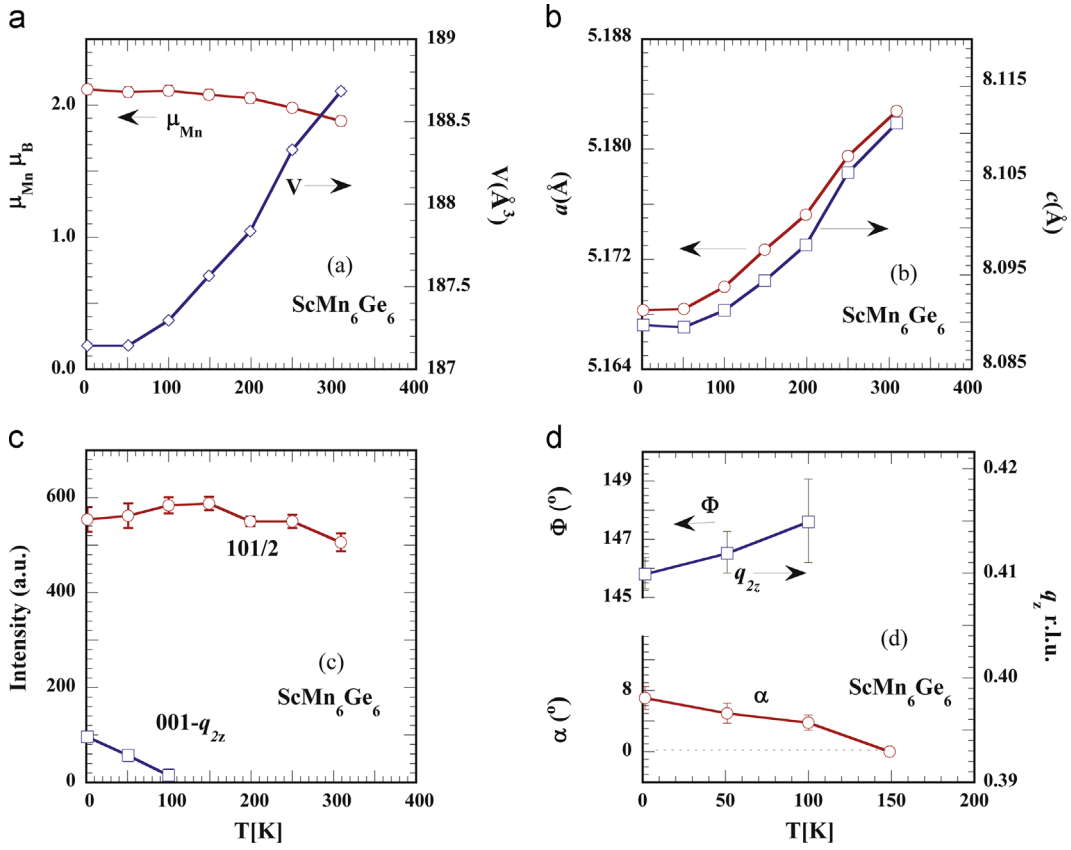

Fig. 6. Temperature dependence of the (a) ordered Mn moment μ_{Mn} and cell volume, (b) *a* and *c* lattice parameters, (c) strongest $\mathbf{q}_1$ intensity (1, 0, 1/2) and the very weak $\mathbf{q}_2$ (001-$\mathbf{q}_2$), and (d) spiral angle $\Phi = 2\pi q_z$ and the cone angle in the *LT* range 1.5–100 K of $ScMn_6Ge_6$.

structure is only stable below 100 K and is described by two vectors $\mathbf{q}_1$, $\mathbf{q}_2$.

The present results compared to the preliminary data given in [9] point to possible sample dependence of the $ScMn_6Ge_6$ behaviour. The differences to our results regard (i) a higher $T_t \approx 250$ K value than ours, (ii) a lower 2θ angle location of the $000 \pm \mathbf{q}_2$ satellite found in [9] suggesting a smaller $\mathbf{q}_2$ value at 1.5 K than ours, and (iii) the strong decrease of the $\mathbf{q}_1$ intensities below T_t is not verified by our data cf. Fig. 6c and d. The *LT* behaviour of $ScMn_6Ge_6$ resembles that of the non-magnetic RMn_6Ge_6, R=Y (q_{2z}=0.385) and R=Lu (q_{2z}=0.402).

3. Concluding remarks

The neutron data obtained in the course of the present investigation for $ScMn_6Ge_6$ are in good agreement with the macroscopic magnetic measurements [3].

The *HT* magnetic ordering is exclusively dominated by the uniaxial antiferromagnetic arrangement over the temperature region, 100–309 K. The Mn ordering within the atomic layers (0 0 1) is ferromagnetic as expected from the high and positive θ_p=500 K value [3]. The sign change of the (0 0 1) ferromagnetic Mn-layers at z=1/4, 3/4, 5/4, 7/4 may be described by the magnetic modes (+ − − +) or (++− −). Neutron diffraction cannot distinguish between these two antiferromagnetic modes, however the observation that the Mn layers sandwiching the *R* layer are close to ferromagnetic coupling at low temperature in the rest of the series, suggest that the (+ − − +) configuration is more probable. The refined deviation of from the $z_{Mn} < 1/4$ value results to unequal distances $d_{Mn(-0.24)-Mn(0.24)} < d_{Mn(0.24)-Mn(1-0.24)}$. This suggests that the shorter distance between the Mn layers sandwiching Sc–Ge2 at z=0 favours ferromagnetism and the larger distance between the Mn layers sandwiching the Ge1–Ge3 favours antiferromagnetism.

The Mn sublattice moment value (2.1–1.9 μ_B) remains nearly constant between 1.5 K and 309 K. $ScMn_6Ge_6$ has the highest ordering T_N temperature of the whole family. As pointed out in Ref. [3] the ordering temperatures within the RMn_6Ge_6 family increases linearly with decreasing R^{3+} size when going from Gd to Lu because the Mn(z=1/4)–Mn(z=3/4) interaction responsible of

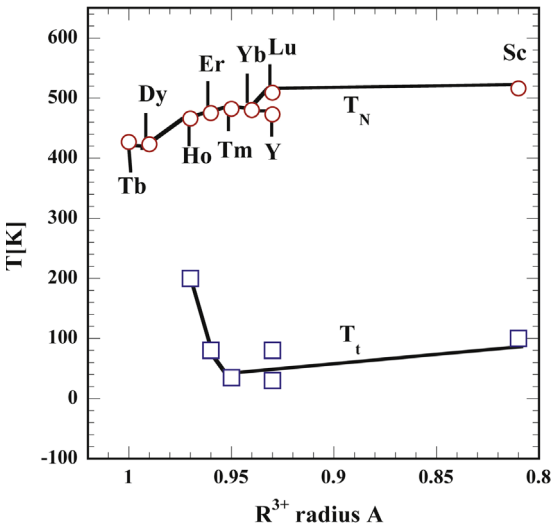

Fig. 7. Ordering T_N temperature and T_t spin reorientation transition temperature as a function of metal radius R^{3+} in the antiferromagnetic compounds RMn_6Ge_6 with $HfMn_6Ge_6$ structure type.

the three dimensional AF ordering increases with decreasing the Mn–Mn distance. The preferred moment direction depends on the thermal variation of the Mn anisotropy.

Fig. 7 shows the ordering temperatures as a function of the R^{3+} ionic radius. For the Ho, Er, Tm, Lu, and Y compounds this interaction should be antiferromagnetic since they all have the same collinear AF ordering type in the *HT* region. It appears that also the stability range of the uniaxial antiferromagnetic structure is linearly dependent on the R^{3+} size. In the Tm compound the collinear structure type was covering the major part of the ordered regime from T_t=35 K to T_N=482 K.

A similar result was for the magnetic rare earth $YbMn_6Ge_6$ and $YbMn_6Ge_{5.7}Sn_{0.3}$ compounds where T_t was found to be 40 K and $\approx$ 55 K [15,16], respectively. The *HT* range 300 K magnetic ordering is again described by a single vector $\mathbf{q}_1=(0, 0, 1/2)$ and exclusively the $\mu_{zMn}=1.69(24)\,\mu_B$ order. Below T_t, Yb orders and is antiferromagnetically coupled to Mn with a complex cone structure $\mathbf{q}_2=(0, 0, q_z)$ the cone axis making an angle with the *c*-axis while the $\mathbf{q}_1$ reflections disappear in favour of the $\mathbf{q}_2$ reflections and a ferromagnetic component evolves.

If the size effect is dominant also in T_t the Yb [15] and the even smaller Sc^{3+} ion should present a lowering of T_t. The present experiment shows that for Sc^{3+} T_t does not drop to zero and it is even higher than for the larger ions YMn_6Ge_6 (80 K) $LuMn_6Ge_6$ (30 K) compounds [9] that have very similar *HT* and *LT* type magnetic structures as $ScMn_6Ge_6$.

The appearance of incommensurate modulated *LT* structure indicates the existence of T-dependent competing antiferromagnetic ferromagnetic Mn–Mn exchange interactions whose strength changes as the Mn–Mn distance changes with *T* and the thermal variation of the anisotropy terms.

References

[1] R.R. Olentich, L.G. Akselrud, Y.a.P. Yarmoliuk, Dopov. Akad. Nauk. Ukr. RSR Ser. A 2 (1981) 84.
[2] E. Parthé, B. Chabot, Handbook on the Physics and Chemistry of Rare Earths, in: K.A. Gschneidner Jr., L. Eyring (Eds.), North-Holland, Amsterdam, 1984, p. 113.
[3] G. Venturini, R. Welter, B. Malaman., J. Alloys Compd. 185 (1992) 99.
[4] P. Schobinger-Papamantellos, G. André, J. Rodríguez-Carvajal, J.H.V.J. Brabers, K.H.J. Buschow., J. Alloys Compd. 226 (1995) 152.
[5] G. Venturini, R. Welter, B. Malaman, J. Alloys Compd. 200 (1993) 51.
[6] P. Schobinger-Papamantellos, G. André, J. Rodriguez-Carvajal, K.H.J. Buschow., J. Alloys Compd. 219 (1995) 176.
[7] P. Schobinger-Papamantellos, J.H.V.J. Brabers, K.H.J. Buschow, J. Magn. Magn. Mater. 139 (1995) 119.
[8] P. Schobinger-Papamantellos, G. André, J. Rodriguez-Carvajal, J.H.V.J. Brabers, K.H.J. Buschow., J. Alloys Compd. 226 (1995) 113.
[9] T. Mazet, R. Welter, G. Venturini, E. Ressouche, B. Malaman, Solid State Commun. 110 (1999) 407.
[10] J.H.V.J. Brabers, V.H.M. Duijn, F.R. de Boer, K.H.J. Buschow, J. Alloys Compd. 198 (1993) 127.
[11] J. Rodríguez-Carvajal, Physica B 192 (1993) 55 (The programs of the FullProf Suite and their corresponding documentation can be obtained from the web ⟨http://www.ill.eu/sites/fullprof/⟩).
[12] L.C. Chapon, J. Rodríguez-Carvajal, FullProf Studio is a program of the FullProf Suite that is freely available from ⟨http://www.ill.eu/sites/fullprof/⟩.
[13] B. Ya, Kotur, E. Gratz, Handbook on the Physics and Chemistry of Rare Earths, in: A. Karl, Jr. Gschneidner, Eyring Le Roy (Eds.), Elsevier, 1999, pp. 339–533.
[14] J. Rodríguez-Carvajal, F. Bourée, Symmetry and magnetic structures, in: Proceedings of the EPJ Web of Conferences 22, 00010, EDP Sciences, 2012, Available at http://www.epj-conferences.org or http://dx.doi.org/10.1051/epjconf/20122200010.
[15] T. Mazet, Thése de Doctorat es Sciences Nancy I, 2000, Nancy.
[16] T. Mazet, H. Ihou-Mouko, D.H. Ryan, C.J. Voyer, J.M. Cadogan, B. Malaman., J. Phys.: Condens. Matter 22 (2010) 116005, http://dx.doi.org/10.1088/0953-8984/22/11/116005 (13pp.).